Valence orbital method of calculating harmonic emission from diatomic molecule*

Wang Yu-Quan(王玉铨)†, Chen De-Ying(陈德应), Xia Yuan-Qin(夏元钦), Fan Rong-Wei(樊荣伟), and Lu Fa-Ming(卢发铭)

National Key Laboratory of Tunable Laser Technology, Harbin Institute of Technology, Harbin 150001, *China*

(Received 16 January 2009; revised manuscript received 14 July 2009)

We present a valence orbital method of calculating high-order harmonic generation from a diatomic molecule with arbitrary orientation by using a space rotation operator. We evaluate the effects of each valence orbital on harmonic emissions from N_2 and O_2 molecules in detail separately. The calculation results confirm the different properties of harmonic yields from N_2 and O_2 molecules which are well consistent with available experimental data. We observe that due to the orientation dependence of σ and π orbitals, the bonding orbital $(\sigma_{2pz})^2$ of N_2 determines the maximum of harmonic emission when the molecular axis of N_2 is aligned parallel to the laser vector, and the magnitude of the high harmonic signal gradually weakens with the orientation angle of molecular axis increasing. But for O_2 molecule the antibonding orbitals $(\pi^*_{2py})^1$ and $(\pi^*_{2pz})^1$ contribute to the maximum of harmonic yield when O_2 is aligned at 45° and bonding orbitals $(\pi_{2py})^2$ and $(\pi_{2pz})^2$ slightly influence the orientation angle of maximum of harmonic radiation not exactly at 45°.

Keywords: harmonic emission, valence orbital, space rotation operator, molecular orientation

PACC: 3280K

1. Introduction

Recent advances including experiments and theories in strong field molecular physics have made it possible to control over the spatial orientation of molecules within the laboratory frame in order to get more insight into chemical reaction dynamics.[1−3] High-order harmonic generation (HHG) from aligned molecules in strong laser fields of femtosecond duration have attracted increasing interest over the past ten years due to its useful applications in the tomographic reconstruction of molecular orbitals,[4] probing molecular vibrational and rotational dynamics,[5,6] and proton dynamics in molecules on an attosecond time scale.[7] In recent years the experimental and the theoretical work on HHG from aligned molecules[8−12] are well developed and mainly impelled by the extra degrees of freedom and the nonspherical symmetry as compared with the case of atoms which may lead to richer physics phenomena and a higher degree modulation of HHG. In controlling high harmonic generation experiment with molecular wave packets, maximum harmonic signal occurs when molecular axis is aligned parallel for N_2 and at around 45° for O_2 to the laser polarization, which suggests that the harmonic emission is influenced by the highest occupied molecular orbitals (HOMO).[13] Simultaneously it is worth while mentioning that theoretical work[14] about HHG from diatomic molecules has obtained good agreement with experimental results where their theoretical model includes nuclear motion and their results show that the alignment dependence of high-harmonics is governed by the symmetry of HOMO. In addition, another work based on strong field approximation discussed the influence of the ground state wave function and laser polarization on HHG from N_2[15,16] and the ionization properties of hydrogen atom exposed to intense laser field.[17] At present, experiments and theories about HHG from diatomic molecules are mainly focusing on the predominant effect of molecular HOMO and ground state wave function, but in our opinion the valence orbitals also play an indispensable role in the multiphoton ionization process of HHG from diatomic molecules. So we assume that in the time of laser pulse–molecule interaction the orientation of molecular axis is at a certain angle with respect to laser polarization ($T_r = 1/(2B_e c) \sim 10^{-12}$ s $\gg T = 2\pi/\omega \sim 10^{-15}$ s) and employ space rotation operator to calcu-

*Project supported by the National Natural Science Foundation of China (Grant Nos. 10774033, 60878018 and 10674036), the Program of Excellent Team in Harbin Institute of Technology, and the Program for New Century Excellent Talents in University (NCET), China (Grant No. NCET-04-0319).

†Corresponding author. E-mail: wyq3369@yahoo.com.cn

© 2010 Chinese Physical Society and IOP Publishing Ltd

late high harmonic spectrum within three-step model (TSM).[18,19] Especially in harmonic generation process of intense laser pulse–molecule interaction, each valence orbital effect on harmonic intensity is evaluated in detail at a different molecular orientation, which gives a reasonable explanation to the phenomena observed in experiments.

2. Theory

The HHG is well understood within the framework of the three-step model. The single active electron approximation (SAE) is a semi-analytical method, in which both the influence of the laser field is neglected when the electron is bound and the systemic binding potential is ignored when the electron is in the continuum state. Theoretically HHG is governed by the Fourier components in the field-dresses wave function. Hence in the dipole approximation the dipole moment, whose Fourier transform determines high harmonic spectrum, is (atomic units are used throughout the paper)

$$d(t) = \langle \Phi_{\rm f}(\boldsymbol{r},t)|\hat{D}_\varepsilon|\Phi_i(\boldsymbol{r},t)\rangle, \tag{1}$$

where $\hat{D}_\varepsilon = \sum_{i=1}^{n} \boldsymbol{\varepsilon}\cdot\boldsymbol{r}_i$ is the dipole operator; $\boldsymbol{r}_i$ is the coordinate of electron i; $\boldsymbol{\varepsilon}$ is the polarization vector of laser field; $\Phi_{\rm i}$ and $\Phi_{\rm f}$ are initial and final states of electron in bound system, dressed by the laser field, respectively. For a diatomic molecule, its wavefunction may be approximated by a linear combination of two atomic obitals in a two-centre binding potential, and the ground state wave function of bonding electron for a diatomic molecule is

$$\varphi_0^z(\boldsymbol{r}) = \frac{1}{\sqrt{2}}\varphi_Z(\boldsymbol{r}+\boldsymbol{R}/2) \pm \frac{1}{\sqrt{2}}\varphi_Z(\boldsymbol{r}-\boldsymbol{R}/2), \tag{2}$$

where the general asymptotic form of $\varphi_Z(r)$ is $\varphi_Z(\boldsymbol{r}) = Ar^{Z/\kappa-1}\exp(-\kappa r)\mathrm{Y}_{lm}(\hat{\boldsymbol{r}})$;[20] $\pm$signs are corresponding to bonding and antibonding orbital wave functions respectively; $\boldsymbol{R}$ is the internuclear distance vector. Here, $\kappa = \sqrt{2|E_{\rm b}|}$ with $E_{\rm b}$ being the field-free ground state eigenenergy; coefficient A is the normalized constant; Z is the charge of the residual nucleus. For high harmonic generation from diatomic molecule analysis, we consider only linearly polarized laser field which is in the following form:

$$\boldsymbol{E}(t) = \boldsymbol{\varepsilon}\cdot E_0 \sin\omega t, \tag{3}$$

where $\boldsymbol{\varepsilon}$ is a unit vector of polarization direction which is chosen to be along the z axis, E_0 is the amplitude of laser field, and ω is the laser frequency. The laser–electron interaction potential is[21]

$$\boldsymbol{V}_{\rm F}(\boldsymbol{r},t) = \boldsymbol{A}(t)\cdot(-\mathrm{i}\nabla) + A^2(t)/2, \tag{4}$$

where $\boldsymbol{A}(t) = -\int_{-\infty}^{t}\boldsymbol{E}(\tau)\mathrm{d}\tau = \boldsymbol{\varepsilon}\cdot A_0\cos\omega t$ is the classical electron momentum. In terms of the three-step picture on the assumption that $\Phi_{\rm i}\equiv\Phi_{\rm f}$ and using Green function propagator we transform $d(t)$ into

$$d(t) = -\mathrm{i}\int_{-\infty}^{t}\mathrm{d}t'\langle\Phi_0(\boldsymbol{r},t)|\hat{D}_{\boldsymbol{\varepsilon}}G(\boldsymbol{r},t;t') \times \boldsymbol{V}_{\rm F}(\boldsymbol{r},t')|\Phi_0(\boldsymbol{r},t')\rangle. \tag{5}$$

Because we suppose that only one active electron is ionized, neglecting the influence of the molecular potential on the electron in continuum of state, the Green function propagator $G(\boldsymbol{r},t;t')$ is represented via the long-wavelength-approximation Volkov solution which is an eigenfunction of $\boldsymbol{V}_{\rm F}(\boldsymbol{r},t)$ operator for a free electron in the laser field and it has the form[21]

$$\Phi_{\boldsymbol{p}}(\boldsymbol{r},t) = [1/(2\pi)^{3/2}]\exp\left[\mathrm{i}\,\boldsymbol{p}\cdot\boldsymbol{r} - \mathrm{i}\,p^2t/2 - \mathrm{i}\int_{-\infty}^{t}\mathrm{d}\tau(\boldsymbol{A}(\tau)\cdot\boldsymbol{p} + A^2(\tau)/2)\right]. \tag{6a}$$

Especially for monochromatic linearly polarized plane wave, the Volkov wave function becomes into

$$\Phi_{\boldsymbol{p}}(\boldsymbol{r},t) = [1/(2\pi)^{3/2}]\exp\left[\mathrm{i}\left(\boldsymbol{p}\cdot\boldsymbol{r} - p^2t/2 - U_pt + \xi\sin\omega t - \frac{U_p}{2\omega}\sin 2\omega t\right)\right], \tag{6b}$$

where $\xi = -A_0\boldsymbol{p}\cdot\boldsymbol{\varepsilon}/\omega$, $U_{\boldsymbol{p}} = A_0^2/4$ is the ponderomotive potential and $\boldsymbol{p}$ denotes the momentum of active electron in continuum state. Subsequently we obtain the following approximation to the dipole moment

$$d(t) = -\mathrm{i}\int_{-\infty}^{t}\mathrm{d}t'\int\mathrm{d}^3\boldsymbol{p}\langle\Phi_0(\boldsymbol{r},t)|\hat{D}_{\boldsymbol{\varepsilon}}|\Phi_{\boldsymbol{p}}(\boldsymbol{r},t)\rangle\langle\Phi_{\boldsymbol{p}}(\boldsymbol{r},t')|\boldsymbol{V}_{\rm F}(\boldsymbol{p},t')|\Phi_0(\boldsymbol{r},t')\rangle, \tag{7}$$

where the operator $-\mathrm{i}\nabla$ in interaction potential $\boldsymbol{V}_{\rm F}(\boldsymbol{r},t)$ is replaced by $\boldsymbol{p}$ and the Fourier transform of the dipole moment is

$$\boldsymbol{d}_N = \frac{1}{T}\int_0^T \mathrm{d}t \exp(\mathrm{i}\,N\omega t) d(t) = -\frac{\mathrm{i}}{T}\int_0^T \mathrm{d}t \int_{-\infty}^t \mathrm{d}t' \int \mathrm{d}^3\boldsymbol{p} \langle \varphi_0^z(\boldsymbol{r})| \exp(\mathrm{i}\,N\omega t)\hat{D}_{\boldsymbol{\varepsilon}}|\Phi_{\boldsymbol{p}}(\boldsymbol{r},t)\rangle$$
$$\times \exp(\mathrm{i}\,E_\mathrm{b}t)\langle \Phi_{\boldsymbol{p}}(\boldsymbol{r},t')|\boldsymbol{V}_\mathrm{F}(\boldsymbol{p},t')|\varphi_0^z(\boldsymbol{r})\rangle \exp(-\mathrm{i}\,E_\mathrm{b}t'). \tag{8}$$

Then employing Eq. (6b), the Bessel function $\exp\left(-\mathrm{i}\,\xi\sin\omega t + \mathrm{i}\,\dfrac{U_p}{2\omega}\sin 2\omega t\right) = \sum\limits_k \mathrm{J}_k(\xi, -U_p/2\omega)\mathrm{e}^{-\mathrm{i}\,kwt}$ and $\mathrm{J}_k(\xi, -U_p/2\omega) = \sum\limits_{n=-\infty}^{\infty} \mathrm{J}_n\left(\dfrac{-U_p}{2\omega}\right) J_{(k-2n)}(\xi)$,[21] we obtain the following expressions

$$\begin{aligned}
&\int_{-\infty}^t \mathrm{d}t' \langle \Phi_{\boldsymbol{p}}(\boldsymbol{r},t')|\boldsymbol{V}_\mathrm{F}(\boldsymbol{p},t')|\varphi_0^z(\boldsymbol{r})\rangle \exp(-\mathrm{i}\,E_\mathrm{b}t') \\
&= \frac{-\mathrm{i}}{(2\pi)^{3/2}}\int_{-\infty}^t \tilde{\varphi}_0^z(\boldsymbol{p}) \exp(\mathrm{i}\,p^2t'/2 - \mathrm{i}\,E_\mathrm{b}t')\mathrm{d}\exp\left(\mathrm{i}\,U_pt' - \mathrm{i}\,\xi\sin\omega t' + \mathrm{i}\,\frac{U_p}{2\omega}\sin 2\omega t'\right) \\
&= \frac{-\mathrm{i}}{(2\pi)^{3/2}}\tilde{\varphi}_0^z(\boldsymbol{p})\Bigg\{\exp(\mathrm{i}\,p^2t'/2 - \mathrm{i}\,E_\mathrm{b}t')\,\exp\left(\mathrm{i}\,U_pt' - \mathrm{i}\,\xi\sin\omega t' + \mathrm{i}\,\frac{U_p}{2\omega}\sin 2\omega t'\right)\Bigg|_{-\infty}^t \\
&\quad - \int_{-\infty}^t \exp\left(\mathrm{i}\,U_pt' - \mathrm{i}\,\xi\sin\omega t' + \mathrm{i}\,\frac{U_p}{2\omega}\sin 2\omega t'\right)\mathrm{d}\exp[\mathrm{i}(p^2/2 - E_\mathrm{b})t']\Bigg\} \\
&= \frac{-\mathrm{i}}{(2\pi)^{3/2}}\tilde{\varphi}_0^z(\boldsymbol{p})\Bigg\{\exp\left[\mathrm{i}(p^2/2 - E_\mathrm{b})t\right]\sum_k \mathrm{J}_k(\xi, -U_p/2\omega)\exp\left[\mathrm{i}\,(U_p - k\omega)\,t\right] \\
&\quad - \mathrm{i}(p^2/2 - E_\mathrm{b})\sum_k \mathrm{J}_k(\xi, -U_p/2\omega)\int_{-\infty}^t \mathrm{d}t' \exp\left[\mathrm{i}\left(p^2/2 - E_\mathrm{b} + U_p - k\omega\right)t'\right]\Bigg\} \\
&= \frac{-\mathrm{i}}{(2\pi)^{3/2}}\sum_k \mathrm{J}_k(\xi, -U_p/2\omega)\tilde{\varphi}_0^z(\boldsymbol{p})\exp\left[\mathrm{i}(p^2/2 - E_\mathrm{b} + U_p - k\omega)t\right]\left(\frac{U_p - k\omega}{p^2/2 - E_\mathrm{b} + U_p - k\omega}\right),
\end{aligned} \tag{9}$$

and

$$\begin{aligned}
\boldsymbol{d}_N &= \frac{-1}{(2\pi)^{3/2}T}\int_0^T \mathrm{d}t \int \mathrm{d}^3\boldsymbol{p}\sum_k \mathrm{J}_k(\xi, -U_p/2\omega)\tilde{\varphi}_0^z(p)\left(\frac{U_p - k\omega}{p^2/2 - E_\mathrm{b} + U_p - k\omega}\right) \\
&\quad \times \exp\left[\mathrm{i}(p^2/2 - E_\mathrm{b} + U_p - k\omega)t\right]\langle \varphi_0^z(\boldsymbol{r})|\exp(\mathrm{i}\,N\omega t)\hat{D}_{\boldsymbol{\varepsilon}}|\Phi_{\boldsymbol{p}}(\boldsymbol{r},t)\rangle \exp(\mathrm{i}\,E_\mathrm{b}t) \\
&= \frac{-1}{(2\pi)^3 T}\sum_k \int \mathrm{d}^3\boldsymbol{p}\left(\frac{U_p - k\omega}{p^2/2 - E_\mathrm{b} + U_p - k\omega}\right)\mathrm{J}_k(\xi, -U_p/2\omega)\tilde{\varphi}_0^z(\boldsymbol{p})\boldsymbol{\varepsilon}\cdot\nabla_{\boldsymbol{p}}[-\mathrm{i}\,\tilde{\varphi}_0^{z*}(\boldsymbol{p})] \\
&\quad \times \int_0^T \mathrm{d}t \exp\left[\mathrm{i}(N\omega t - k\omega t + \xi\sin\omega t - \frac{U_p}{2\omega}\sin 2\omega t)\right] \\
&= \frac{-\mathrm{i}\,\pi}{(2\pi)^3 T}\sum_k p_k \int \mathrm{d}O_{p_k}\,(U_p - k\omega)\,\mathrm{J}_k(\xi_{p_k}, -U_p/2\omega)\,(\tilde{\varphi}_0^z(\boldsymbol{p})\boldsymbol{\varepsilon}\cdot\nabla_{\boldsymbol{p}}[-\mathrm{i}\,\tilde{\varphi}_0^{z*}(\boldsymbol{p})])\,|_{\boldsymbol{p}=p_k} \\
&\quad \times \int_0^T \mathrm{d}t \exp\left[\mathrm{i}(N\omega t - k\omega t + \xi_{p_k}\sin\omega t - \frac{U_p}{2\omega}\sin 2\omega t)\right],
\end{aligned} \tag{10}$$

where $\tilde{\varphi}_0^z(\boldsymbol{p}) = \int \mathrm{d}^3r \exp(-\mathrm{i}\,\boldsymbol{p}\cdot\boldsymbol{r})\varphi_0^z(\boldsymbol{r})$ is the Fourier transform of $\varphi_0^z(\boldsymbol{r})$ and polar approximation

$$\int_0^\infty \frac{f(\boldsymbol{p})\,\mathrm{d}\left(\boldsymbol{p}^2/2\right)}{(\boldsymbol{p}^2/2 - E_\mathrm{b} + U_p - k\omega) \mp \mathrm{i}\,\varepsilon} = \pm\,\mathrm{i}\,\pi f(p_k)$$

is adopted with $p_k = \sqrt{2\,(k\omega + E_\mathrm{b} - U_p)}$.

The initial condition of molecule includes angle β of molecular axis with respect to z axis and the valence orbital wave function in the body-fixed frame. According to Refs. [14], [18] and [22] the dominant contribution to the harmonic emission comes from the electrons which tunnel away but then recombine with molecule, which implies that those electrons with momenta parallel to laser vector are most likely to recombine with molecule. Thus if we consider only the electrons with $\boldsymbol{p}$ parallel to laser polarization (z axis), $\tilde{\varphi}_0^z(\boldsymbol{p})$ will reduce into integral[23]

$$\tilde{\varphi}_0^z(\boldsymbol{p}) = \frac{1}{p}\sqrt{\frac{2}{\pi}}\int_0^\infty \varphi_0^z(r)\sin(pr)r\mathrm{d}\boldsymbol{r}. \quad (11)$$

In order to calculate integral $\tilde{\varphi}_0^z(\boldsymbol{p})$, using space rotation operator, $\mathrm{Y}_l^m(\hat{\boldsymbol{r}})$ can be expanded into a series space spherical functions from body-fixed frame to space-fixed coordinate system as follows:

$$\mathrm{Y}_{lm}(\hat{\boldsymbol{r}}) = \sum_{m'} D^l_{m',m}(\vartheta)\mathrm{Y}_{lm'}(\beta) \quad (12)$$

with $D^l_{m'm}(\alpha,\beta,\gamma) = d^l_{m'm}(\beta)\exp[-\mathrm{i}(m'\alpha + m\gamma)]$. The Euler angles $\vartheta(\alpha,\beta,\gamma)$ characterize the molecule rotation related to z axis. $D(\vartheta)$ denotes the matrix elements of the rotation operator. Because a linear diatomic molecule has two degrees of freedom in space, the Euler angle γ is redundant with an arbitrary value and we set the phase angle $\alpha = 0$ for simplifying the problem, therefore three parameters of orientation will reduce into a single angle (β). $d^l_{m'm}(\beta) = \langle lm'|\exp(-\mathrm{i}\beta J_y)|lm\rangle$, and J_y is angular momentum component in the laboratory frame. Using the matrix of J_y, we can represent $d^l_{m'm}(\beta)$ by a finite polynomial with variable of $\beta/2$[24] and the rotation of a molecule in space is determined mainly by the angle β between the molecular axis and laser vector.

According to Ref. [23] $\tilde{\varphi}_0^z(\boldsymbol{p})$ can be represented by the following form for number j valence orbital wave function (for bonding valence orbital):

$$\tilde{\varphi}_0^{z,j}(\boldsymbol{p}) = A\sqrt{2/\pi}\cos(pR\cos\beta/2)\frac{\Gamma(1+Z/\kappa)\sin[(1+Z/\kappa)\arctan(p/\kappa)]}{p(p^2+\kappa^2)^{(1+Z/\kappa)/2}}\sum_{m'} D^l_{m',m}(\vartheta)\mathrm{Y}^j_{lm'}(\beta). \quad (13)$$

In particular, for a neutral molecule ($Z = 0$)

$$\tilde{\varphi}_0^{j}(\boldsymbol{p}) = A\sqrt{2/\pi}\cos(pR\cos\beta/2)\frac{1}{p(p^2+\kappa^2)}\sum_{m'} D^l_{m',m}(\vartheta)\mathrm{Y}^j_{lm'}(\beta). \quad (14)$$

Therefore the estimation of the N-th harmonic from diatomic molecule with arbitrary orientation β with respect to z axis is

$$\begin{aligned}\boldsymbol{d}_N = {} & \frac{-\mathrm{i}\,\pi}{(2\pi)^3 T}\sum_j\sum_k p_k\int \mathrm{d}O_{p_k}\,(U_p - k\omega)\,\mathrm{J}_k(\xi_{p_k}, -U_p/2\omega)\left(\tilde{\varphi}_0^{z,j}(\boldsymbol{p})\boldsymbol{\varepsilon}\cdot\nabla_{\boldsymbol{p}}[-\mathrm{i}\,\tilde{\varphi}_0^{z,j*}(\boldsymbol{p})]\right)|_{\boldsymbol{p}=p_k} \\ & \times\int_0^T \mathrm{d}t\exp\left[\mathrm{i}(N\omega t - k\omega t + \xi_{p_k}\sin\omega t - \frac{U_p}{2\omega}\sin 2\omega t)\right]. \end{aligned} \quad (15)$$

For the sake of performing a comparison with the experimental results we need the time-dependent expectation values of the molecular axis orientation angle β[25,26]

$$\langle\cos^2\beta\rangle = \langle\psi(t)|\cos^2\beta|\psi(t)\rangle = \sum_{J,J'\geq|M|} F_J^*(t)F_{J'}(t)\langle JM|\cos^2\beta|J'M\rangle, \quad (16)$$

where molecular rotation wave packet is expressed as the superposition of a series of field-free rotor spherical harmonics $\psi(t,\beta) = \sum_{J'\geq|M|} F_{J'}(t)|JM\rangle$, and the coefficients $F_J(t)$ are obtained by solving a set of coupled linear equations[27−29] as follows:

$$\begin{aligned}\frac{\mathrm{i}\,\hbar}{B_\mathrm{e}}\dot{F}_J(t) = {} & [E_J/B_\mathrm{e} - f(t)^2\omega_\perp(t)]F_J(t) - f(t)^2\Delta\omega(t)\sum_{J'}F_{J'}(t)\langle JM|\cos^2\beta|J'M\rangle \\ & - \frac{1}{B_\mathrm{e}}\mu_0 E(t)f(t)\sum_{J'}F_{J'}(t)\langle JM|\cos\beta|J'M\rangle, \end{aligned} \quad (17)$$

where the initial condition of $F_J(t)$ is subject to the initial temperature of molecules with a statistical Boltzmann factors $F_J(0) = \delta_J(t)\exp[-J(J+1)/\gamma]/Q_\mathrm{r}$ where $\gamma = kT/B_\mathrm{e}$ is the reduced rotational temperature and $Q_\mathrm{r} \cong T/(\delta\Theta_\mathrm{r})$ is the rotational partition function, with Θ_r being the characteristic rotational temperature, (in the case of diatomic molecules $\delta = 1$ for hetero-nuclear and $\delta = 2$ for homo-nuclear). Then the time-dependent amplitude of the N-th harmonic emission is $d_N(\bar{\beta}(t))$.

3. Results and discussion

In this section we present a calculation about valence orbitals for the HHG yield from N_2 and O_2 molecules with arbitrary orientation exposed to a linearly polarized laser field. The intensity of femtosecond laser pulse with a wavelength of 800 nm is selected to be suitable for single electron ionization case. This numerical procedure of the HHG process has a finite number $k_{\max} = 2U_p/\omega + k_0$ corresponding to effective number $k = k_{\max} - k_0$ of open above-threshold ionization (ATI) channels actually contributing to the total amplitude of the N-th high harmonic peak.[30] $k_0 = (I_p + U_p)/\omega + 1$, and I_p is the ionization potential. Figure 1 shows the relative strength of the high harmonic yield from N_2 and O_2 molecules as a function of the orientation of molecule, where β is the angle between molecular axis and the laser polarization. As seen from Fig. 1, all orders of high harmonic yield from N_2 have the peak value of the strength with the parallel alignment ($\beta = 0°$) and have the minimum with the perpendicular alignment ($\beta = 90°$). The magnitudes of the harmonic emissions gradually weaken as the orientation angle of molecular axis increases. For O_2 molecule the strongest harmonic yields occur near $\beta = 45°$ and the orientation angles of harmonic peaks each are slightly different from those of other harmonics due to the combinative effect of its bonding orbitals and antibonding orbitals. All these results confirm the experimental observation in Ref. [13].

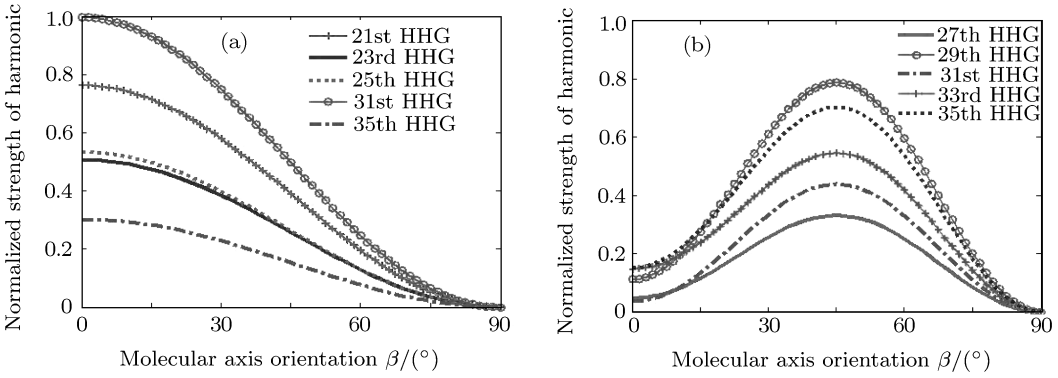


Fig. 1. Orientation dependence of harmonic generation in plateau region from N_2 molecule with equilibrium internuclear distance where the strength of HHG is normalized to 31st harmonic (a) and from O_2 molecule where the strength of HHG is normalized to 29th harmonic (b). The intensity of femtosecond pulse is $I = 2.3 \times 10^{14}$ W/cm^2.

The orientation properties of harmonic emissions from N_2 and O_2 can be explained by the distinct valence orbitals of two molecules. It can be seen from Fig. 2 that different contributions of valence orbitals to HHG from N_2 and O_2 result in their distinct orientation dependence of HHG. For N_2 the valence bond orbitals are $(\pi_{2px})^2, (\pi_{2py})^2$ (the projection of the total angular momentum on z axis $\Lambda = 1$) and $(\sigma_{2pz})^2$ ($\Lambda = 0$). The $(\sigma_{2pz})^2$ bonding orbital essentially dominates the process of harmonic emission because at $\beta = 0°$ the molecular axis aligned parallel to the laser electric field and the coherent superposition of $(\sigma_{2pz})^2$ bonding orbital wave function and Volkov wave function with continuum electron propagating in the direction of laser polarization induce a parallel dipole moment and lead dipole oscillation to speed up, thereby obtaining the strong harmonic yield. Compared with $(\sigma_{2pz})^2$, both $(\pi_{2px})^2$ and $(\pi_{2py})^2$ bonding orbitals are inversely symmetric with respect to the internuclear axis plane. When the molecular axis is perpendicular to laser field vector (the propagating direction of the recombination electron), the induced dipole moment in the direction perpendicular to the laser polarization plane is suppressed by the inverse coherent superposition of two $(\pi_{2p})^2$ bonding orbitals, and harmonic yield from the perpendicular direction is very weak. But at about $\beta = 45°$ the induced dipole component is well strengthened due to the shape of $(\pi_{2p})^2$ bonding orbitals and the harmonic emission is moderately enhanced. Therefore when molecular axis of N_2 is aligned along the laser vector the $(\sigma_{2pz})^2$ bonding orbital essentially determines the maximum of harmonic signals. For O_2 molecule the valence orbitals are $(\sigma_{2px})^2, (\pi_{2py})^2, (\pi_{2pz})^2, (\pi^*_{2py})^1, (\pi^*_{2pz})^1$ and among them two antibonding orbitals $(\pi^*_{2py})^1$ and $(\pi^*_{2pz})^1$ play a dominant role in high-order harmonic generation as shown in Fig. 2. Owing to the midpoint of molecular internuclear axis selected as the origin of coordinates axes the coherent superposition term of antibonding orbital

wavefunction in Eqs. (13) and (14) becomes $\cos(pR\cos\beta/2)$, and $(\pi^*_{2p})^1$ antibonding orbital has a maximum signal exactly at $\beta = 45°$. Although O_2 molecule also has the same $(\sigma_{2px})^2$ bonding orbital as N_2 molecule, its contribution to the high harmonic is much weaker than that from the antibonding orbital $(\pi^*_{2p})^1$ and does not influence the maximum of harmonic emission from O_2 molecule. So, the bonding orbital $(\sigma_{2px})^2$ determines only the amplitude of harmonic signals with the parallel alignment of O_2. The bonding orbitals $(\pi_{2py})^2$ and $(\pi_{2pz})^2$ have similar properties to those of N_2 and each has an obvious effect on the exact position of peak value near $\beta = 45°$. Thus the superposition of all the bonding and antibonding orbitals yields the orientation property of HHG from O_2 molecule. In summary, for O_2 molecule, the antibonding orbitals $(\pi^*_{2py})^1$ and $(\pi^*_{2pz})^1$ contribute maximum of harmonic and two bonding orbitals $(\pi_{2py})^2$ and $(\pi_{2pz})^2$ influence the exact orientation angle of maximum of harmonic.

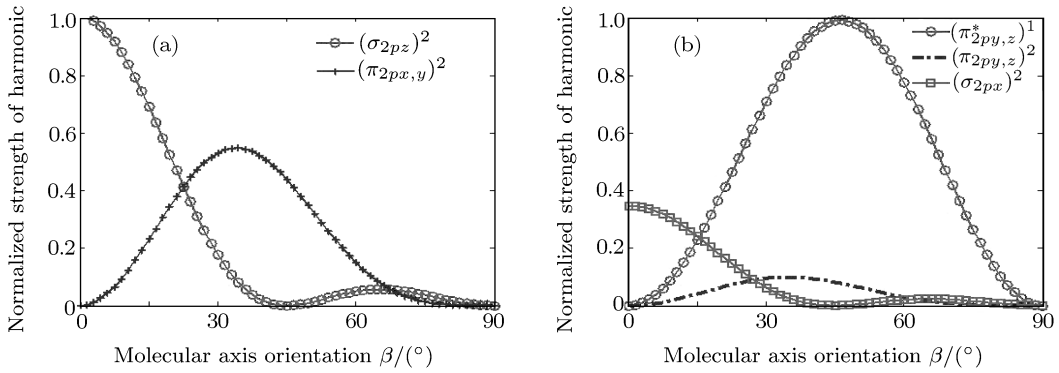


Fig. 2. Different contributions of valence orbitals to the 37th harmonic emission from N_2 molecule (a) and O_2 molecule (b) with arbitrary orientation, with all curves of harmonic yield normalized to unit.

Finally we make a comparison between theoretical results and pump-probe experiment in cases of N_2 and O_2 as presented in Fig. 3 and we observe a good agreement between theory and experiment.

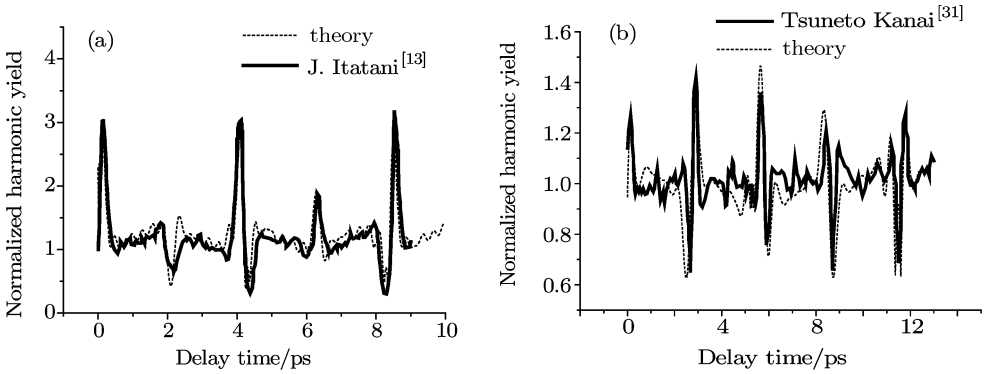


Fig. 3. Comparison between theoretical calculations and the results of pump-probe experiment in the cases of N_2 and O_2. In panel (a) the rotational temperature of N_2 is 30 K, the intensities of pump and probe pulses are 4×10^{13} W/cm^2 and 2×10^{14} W/cm^2 respectively, and in panel (b) the rotational temperature of O_2 is 80 K, and the intensities of pump and probe pulses are 6×10^{13} W/cm^2 and 2×10^{14} W/cm^2 respectively.

4. Conclusion

We present a valence orbital calculation method for HHG from a diatomic molecule with arbitrary orientation by using a space rotation operator. From the numerical results we obtain the orientation property of HHG from N_2 and O_2 molecules. The agreement between experiments and theory is very good, which can be demonstrated successfully by the coherent superposition of each distinct valence orbital. Due to the special orientation dependence of σ and π orbitals, the harmonic emissions from N_2 are much different from those from O_2, which is indicated by calculating each relevant valence orbital in detail. For the N_2 molecule, contribution

from $(\sigma_{2pz})^2$ bonding orbital is the dominant component in harmonic amplitude, and for O_2 molecule, two antibonding orbitals $(\pi^*_{2py})^1$ and $(\pi^*_{2pz})^1$ contribute maximum of harmonic and two bonding orbitals $(\pi_{2py})^2$ and $(\pi_{2pz})^2$ influence the exact orientation angle of maximum of HHG. These results enable one to better understand the importance of valence orbitals in high-order harmonic generation from molecule with arbitrary orientation and serve as a new way to control harmonic and subsequently probe the instantaneous structure of molecular systems.

References

[1] Stapelfeldt H and Seideman T 2003 *Rev. Mod. Phys.* **75** 543

[2] Sakai H, Safvan C P, Larsen J J, Hilligsøe K M, Hald K and Stapelfeldt H 1999 *J. Chem. Phys.* **110** 10235

[3] Rosca-Pruna F and Vrakking M J J 2002 *J. Chem. Phys.* **116** 6579

[4] Itatani J, Levesque J, Zeidler D, Niikura H, Pe'pin H, Kieffer J C, Corkum P B and Villeneuve D M 2004 *Nature* (London) **432** 867

[5] Lein M 2005 *Phys. Rev. Lett.* **94** 053004

[6] Ramakrishna S and Seideman T 2007 *Phys. Rev. Lett.* **99** 113901
Ramakrishna S and Seideman T 2008 *Phys. Rev.* A **77** 053411

[7] Baker S, Robinson J S, Haworth C A, Teng H, Smith R A, Chirila C C, Lein M, Tisch J W G and Marangos J P 2006 *Science* **312** 424

[8] Chen Y, Li Y, Yang S and Liu J 2008 *Phys. Rev.* A **77** 031402

[9] Patchkovskii S, Zhao Z X, Brabec T and Villeneuve D M 2007 *J. Chem. Phys.* **126** 114306

[10] Lan P F and Lu P X 2008 *Phys. Rev.* A **77** 013405

[11] Levesque J, Mairesse Y, Dudovich N, Pepin H, Kieffer J C, Corkum P B and Villeneuve D M 2007 *Phys. Rev.* A **75** 051403(R)

[12] Madsen C B, Mouritzen A S, Kjeldsen T K and Madsen L B 2007 *Phys. Rev.* A **76** 035401

[13] Itatani J, Zeidler D, Levesque J, Spanner M, Villeneuve D M and Corkum P B 2005 *Phys. Rev. Lett.* **94** 123902

[14] Madsen C B and Madsen L B 2006 *Phys. Rev.* A **74** 023403

[15] Guo Z H and Zhou X X 2008 *Acta Phys. Sin.* **57** 1616 (in Chinese)

[16] Cui L, Gu B, Hu Y J, Teng Y Y, Zeng X H and Zhao J 2006 *Acta Phys. Sin.* **55** 4691 (in Chinese)

[17] Jin C, Zhao S F and Zhou X X 2006 *Acta Phys. Sin.* **55** 4078 (in Chinese)

[18] Lewenstein M, Balcou P, Ivanov Y M, L'Huillier A and Corkum P B 1994 *Phys. Rev.* A **49** 2117

[19] Corkum P B 1993 *Phys. Rev. Lett.* **71** 1994

[20] Gribakin G F and Kuchiev M Y 1997 *Phys. Rev.* A **55** 3760

[21] Howard R Reiss 1980 *Phys. Rev.* A **22** 1786

[22] Kuchiev M Y and Ostrovsky V N 1999 *Phys. Rev.* A **60** 3111

[23] Gradshteyn I S and Ryzhik I M 2000 *Table of Integrals, Series and Products* (Sixth Edition) (Beijing: Science Press) pp. 1110–1112

[24] Zare R N 1988 *Angular Momentum: Understanding Spatial Aspects in Chemistry and Physics* (New York: John Wiley and Sons Press) p. 89

[25] Ortigoso J, Rodríguez M, Gupta M and Friedrich B 1999 *J. Chem. Phys.* **110** 3870

[26] Seideman T 1997 *J. Chem. Phys.* **106** 2881

[27] Chen D Y, Wang Y Q, Xia Y Q, Fan R W and Zhang S 2009 *Chin. Phys.* B **18** 3850

[28] Dion C M, Keller A, Atabek O and Bandrauk A D 1999 *Phys. Rev.* A **59** 1382

[29] Torres R, Nalda R D and Marangos J P 2005 *Phys. Rev.* A **72** 023420

[30] Usachenko V I and Pazdzersky V A 2004 *Phys. Rev.* A **69** 013406

[31] Kanai T, Minemoto S and Sakai H 2005 *Nature* (London) **435** 26